

## Damping Investigations of a Simplified Frictional Shear Joint

David O. Smallwood  
Danny L. Gregory  
Ronald G. Coleman

Engineering Sciences Center  
Sandia National Laboratories\*  
PO Box 5800  
Albuquerque, NM 87185  
(505) 844-9743

The inability to include accurate damping models for bolted connections limits the accuracy of structural models to predict dynamic response. Experiments utilizing a system simulating a bolted shear joint to investigate frictional damping associated with micro-slip are discussed. Measurement and three computational techniques to quantify the energy dissipation as a function of the applied force to the shear joint are described. Parameters of the shear joint include the normal force amplitude and distribution, input force, frequency, material type, and surface characteristics. An underlying power law relationship between the energy dissipated per cycle and the applied input force is revealed and explored for the simplified shear joint. Methods to directly observe and measure the damping force at resonance are also discussed. This is a continuation of the work that was presented last year.

### INTRODUCTION

The dynamics of structures with bolted interfaces continue to challenge the ability of analytical models to predict the structural response of these complex systems. The inclusion of the physics associated with the bolted interfaces introduces several potentially non-linear mechanisms that must be modeled for these systems. In particular, the damping (energy dissipation) associated with the bolted interfaces has proved very difficult to model accurately. An experimental program to investigate the microslip phenomenon in bolted interfaces has been initiated at Sandia National Laboratories. An experimental apparatus, described in last year's paper, was designed to isolate a single frictional interface with the parameters of the interface adjustable over selected ranges. For a shear joint with a single bolt, there are multiple slip interfaces between the head of the bolt, washers, and the structural members. Each of these slip interfaces potentially has different surface tractions, material types, surface properties, and contact areas. This complexity was the motivation to devise an experiment where the number of slip interfaces could be reduced to one such that the physics could be more easily isolated. Experiments with the apparatus, utilizing sinusoidal excitation to measure the energy loss per cycle in a manner similar to that reported by other investigators [1-10] were performed. Results from these experiments have revealed insight into the physics associated with the microslip phenomenon and the resulting damping mechanisms. These experiments also exposed several pitfalls to avoid in making accurate measurements of the energy loss per cycle for microslip in a simulated bolted interface. A description of the experiments and discussion of the results follow.

### THE EXPERIMENT

The experimental setup is essentially the same as reported last year [13]. A sketch is shown as Figure 1. The concept is for an experiment with a single shear joint. The joint is preloaded with a line load using cables through rollers. The cable loads are monitored with load cells to assure repeatable surface loading conditions.

\*--Sandia is a multiprogram laboratory operated by Sandia Corporation, a Lockheed Martin Company, for the United States Department of Energy under Contract DE-AC04-94AL85000.

## **DISCLAIMER**

**This report was prepared as an account of work sponsored by an agency of the United States Government. Neither the United States Government nor any agency thereof, nor any of their employees, make any warranty, express or implied, or assumes any legal liability or responsibility for the accuracy, completeness, or usefulness of any information, apparatus, product, or process disclosed, or represents that its use would not infringe privately owned rights. Reference herein to any specific commercial product, process, or service by trade name, trademark, manufacturer, or otherwise does not necessarily constitute or imply its endorsement, recommendation, or favoring by the United States Government or any agency thereof. The views and opinions of authors expressed herein do not necessarily state or reflect those of the United States Government or any agency thereof.**

## **DISCLAIMER**

**Portions of this document may be illegible in electronic image products. Images are produced from the best available original document.**

DEC 19 2000

The rollers are designed to roll on the specimen surface to minimize losses at the roller specimen interface. The bottom roller was also machined with a large radius along the axis of the applied load to generate essentially a point load between the roller and the inertial mass. This was necessary to correct for any alignment problems between the inertial mass and the fixed portion of the specimen. A typical specimen pair is shown as Figure 2. The results reported last year used a specimen pair with a raised face in the contact area. This produces an approximation of a uniform interface pressure. The specimens used for the results in this paper were flat. This resulted in a contact pressure surface more representative of that expected from a bolt. The pressure is maximum under the line load, and decreases as the location moves away from the line load similar to that in the vicinity of a bolt head.

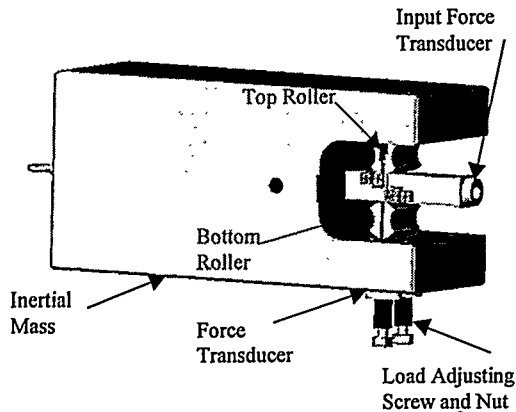


Figure 1. Basic Concept for Single Friction Interface

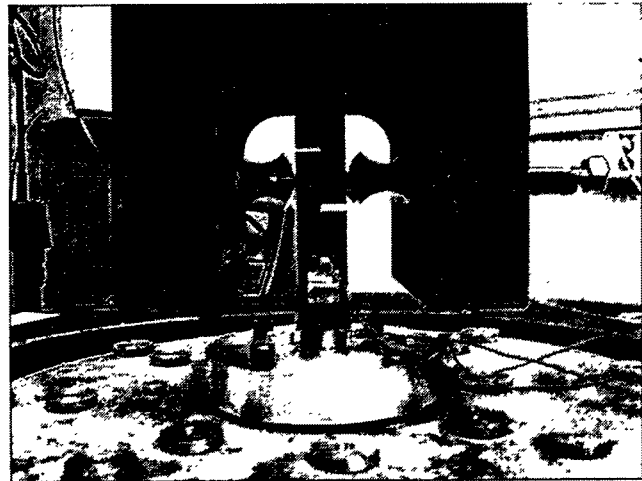


Figure 2. Experimental Setup

The inertial mass was supported with soft steel springs. The highest resonance of the suspension system was about 2 Hz. An oscillatory load shear load was applied through the interface with an electrodynamic shaker.

A finite element model of the experiment was constructed and is reported in another paper [14]. The model proved to be very useful in refining the experiment and interpreting the results.

The force vs. relative displacement was almost a straight line along the stiffness curve with very little apparent area. This created difficulties measuring the relative acceleration when the system was not at resonance. For this reason almost all measurements reported in the paper were measured at the fixed base resonance of the system (near 340 Hz). At the fixed base resonance the input acceleration becomes very small. We found that very small contributions from modes far removed from the driving frequency had large effects on the measurements of the base input acceleration. To minimize the effects of these modes the accelerometer measuring the input motion was moved to a point coincident with the force. The input accelerometer is mounted on the bolt directly under the force gage. The primary measurements for the results reported in this paper are the input force, the coincident input acceleration (the base motion), and the acceleration of the top inertial mass. The accelerometer on the inertial mass was also placed as near the centerline of the experiment as possible to reduce the contributions of unwanted bending and rocking modes.

We also fabricated a solid bar with the same geometry as the friction specimens except there was no friction interface. We frequently used this bar in the test setup as a sanity check. Any energy dissipation or nonlinear response measured with the solid bar must be losses not associated with the joint or experimental error. The solid bar experimental results were quite linear with very low damping.

## METHODS FOR MEASURING ENERGY DISSIPATION

### 1. Measuring the energy loss by finding the area within the force/relative-displacement hysteresis loop

The traditional way to measure energy loss for harmonic motion in the literature of frictional joints is to measure the area within the closed plot (hysteresis plot) of force vs. relative-displacement. An example is shown in Figure 10.

### 2. Measuring the energy loss by looking at the power supplied at the base

The energy dissipated for steady state response in a single input passive system must be equal to the energy supplied at the input to the system to sustain the steady state response. For a simple harmonic input the input energy is

$$U = FX \sin \phi \quad (1)$$

where  $F$  is the magnitude of the force input,  $X$  is the magnitude of the base displacement and  $\phi$  is the phase angle between the force and displacement. The relationship between the magnitude of the acceleration and the magnitude of the displacement is just

$$A = -\omega^2 X \quad (2)$$

Only the component of displacement out of phase with the force will dissipate energy. At resonance

$\sin \phi = 1$ . The orthogonality of sine and cosine functions assures that if either the force or acceleration is a pure sinusoid, then harmonic distortion in the other measure will not dissipate energy. Only the fundamental component will dissipate energy. If both measures are distorted then the harmonics can dissipate energy. Typically this was a small effect. For most of our experiments the force input generated by the electrodynamic shaker had little harmonic distortion. At resonance almost all the harmonic distortion observed was in the base acceleration waveform. The inertial mass acceleration waveform was nearly a scaled version of the base input force.

### 3. Measuring the energy loss/cycle, $U$ , by measuring $Q$

The transmissibility of a viscous damped base excited single degree of freedom system is given by the well known equation [11]

$$T = \frac{1 + (2\zeta\omega/\omega_n)^2}{\sqrt{(1 - \omega^2/\omega_n^2)^2 + (2\zeta\omega/\omega_n)^2}} \quad (3)$$

At the undamped resonant frequency,  $\omega/\omega_n = 1$  and for  $\zeta \ll 1$  the transmissibility is approximately

$$T \approx 1/2\zeta \quad (4)$$

For this discussion the motion measures of interest are the acceleration of the base and mass. For this system the force at the base is just the mass acceleration multiplied by the mass. Therefore the driving point acceleration (base acceleration / base force) is the reciprocal of the transmissibility scaled by the mass.

The transmissibility at resonance is called the amplification factor or quality factor,  $Q$ , ( $Q = T(\omega_n) = 1/2\zeta$ ) of the system. The damping factor is related to the viscous damping coefficient by

$$c = 2m\zeta\omega_n \quad (5)$$

For forced harmonic motion Thomson [12] defines an equivalent viscous damping for systems with other types of damping on the basis of an equivalent energy dissipated per cycle.

$$U = \pi c_{eq} \omega X^2 \quad (6)$$

Which gives

$$U = \frac{\pi m A^2}{Q \omega_n^2} \quad (7)$$

The log of this equation gives

$$\log Q + \log U = \log(\pi m / \omega_n^2) + 2 \log A \quad (8)$$

Therefore for the linear case where  $Q$  is a constant independent of input amplitude, the slopes on a log-log plots of  $Q$  vs.  $A$  is zero, and  $U$  vs.  $A$  is two.

$$\frac{d(\log U)}{d(\log A)} = 2, \text{ for a linear system} \quad (9)$$

Now consider the case where  $Q$  is a function of  $A$ , but a log-log plot of  $Q$  vs.  $A$  is still a straight line with a slope,  $-n$

$$Q = K A^{-n} \quad (10)$$

Taking the log of both sides gives

$$\log Q = \log K - n \log A \quad (11)$$

or

$$\frac{d(\log Q)}{d(\log A)} = -n \quad (12)$$

If the equivalent viscous damping is used instead of  $Q$  the results are

$$\frac{d(\log \zeta)}{d(\log A)} = n \quad (13)$$

Combining Eq. 8 and 11, and differentiating gives

$$\frac{d(\log U)}{d(\log A)} = 2 + n \quad (14)$$

For example, if the slope of  $\zeta$  vs.  $A$  on a log-log plot is +1, the slope of the energy dissipated/per cycle will have a slope of +3.

Plotting  $Q$  or  $\zeta$  vs.  $A$  instead of  $U$  vs.  $A$  gives better insight for two reasons. First a linear system plots as a horizontal line, easy for the eye to observe. Second the data are compressed and fewer decades of data are typically required on the ordinate.

$Q$  is determined directly from the transmissibility, which is measured using a sine sweep test through the resonance. If the waveforms are distorted, measurement of  $Q$  typically looks at only the fundamental component, which is the component that dissipates energy.

We have used all three methods discussed above to measure energy dissipation. When properly applied all three gave essentially the same result. Most of the data reported in this report were determined by measuring  $Q$ .

### THE DAMPING FORCE

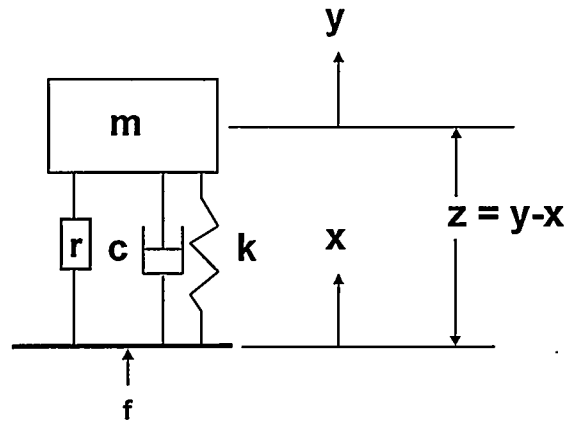


Figure 3 Base Excited Single Degree of Freedom System

The experiment can be represented as a base driven single-degree-of-freedom system as shown in Figure 3. The inertial mass is the mass,  $m$ , and the base is driven by the force,  $f$ . A linear spring,  $k$ , and a linear damping element,  $c$ , represent the linear part of the specimen. The nonlinearities are lumped into the element  $r$ . Thompson [12, Sec.3.7] shows that for a linear single degree of freedom system a plot of force vs. relative displacement,  $z$ , will plot as an ellipse. The major axis will fall on the linear stiffness line. The input force,  $f$ , is the same force that drives the mass,  $m$ . If the force is a sinusoid, the force and the acceleration of the mass will be in phase. The force and displacement of the mass,  $y$ , will be  $180^\circ$  out of phase. The relative displacement will consist of three components, a coincident component (either  $0$  or  $180^\circ$ ), a quadrature component ( $90$  or  $270^\circ$ ) and the harmonic distortion. The quadrature component will be represented by the quadrature component of the fundamental part of the base motion. Generally for linear lightly damped systems the linear stiffness term,  $k$ , will dominate and the hysteresis curve of force vs. relative-displacement will look like a narrow ellipse with the major axis on the linear stiffness line. For a nonlinear system the ellipse will be distorted. Integration of this curve to derive the energy loss is difficult because small errors in phase between the force and relative displacement result in large errors in the energy loss. If the system is driven at the fixed base resonant frequency the phase between the fundamental component of the base displacement and the force or mass displacement is  $90^\circ$ ; the linear elastic term vanishes. The base displacement then represents the dissipative fraction of the motion. If only the fundamental component of the base motion is plotted the hysteresis curve represents the equivalent viscous damping. For a sinusoidal force the harmonic terms of the base displacement do not dissipate energy.

The system can also be viewed as a passive system being driven from the base. The energy dissipated in the joint (the only significant energy loss in the experiment) must be supplied through the base motion. When the input force is plotted as a function of base displacement, the area within the curve represents the input energy. The area within the curves (force vs. relative displacement, force vs. base motion, force vs. fundamental-part-of-base-motion) are all the same.

It is useful to subtract all the linear terms from the base displacement waveform. At resonance this is the displacement at the fundamental. The harmonic motion with the fundamental removed represents the nonlinear portion of the response. Future work will look closely at this fraction of the response.

## DATA REDUCTION

The data were reduced by assuming the data were periodic with a fundamental frequency equal to the driving frequency. A least squares fit of the fundamental and harmonics (typically about seven harmonics were sufficient) were fit to the data. The acceleration and force time histories were then reconstructed from the fit. The velocity and displacement waveforms were constructed by converting the fundamental and harmonic coefficients to velocity and displacement and constructing the velocity and displacement waveforms. This procedure removed most of the noise from the data. The total harmonic distortion in the force was typically about 1%.

## EXPERIMENTAL RESULTS

Experiments were performed to measure the energy loss per cycle for a sinusoidal input force over a range of loads of 60, 120, 180, 240, and 320 lb-peak, with a range of normal forces of 800, 1200, 1600, and 2000 lb. The experimental apparatus was configured with an Unholtz-Dickie T1000 electrodynamic shaker system. The specimens were machined out of 4340 steel with a surface roughness of approximately 32 micro-inch rms. Data were also collected for a geometrically identical solid bar with no frictional interface to establish a lower limit for the unaccounted loss mechanisms in the setup. The energy loss per cycle was experimentally determined by first performing a sine sweep controlling the force at a constant value over a frequency bandwidth encompassing the fixed base resonance of the test apparatus. The fixed base resonant frequency of the system ranged from 330 to 340 Hz depending on the normal clamping load and excitation level. The amplification factor (transmissibility) between the acceleration of the mass to the acceleration of the base was then calculated to determine the amplification factor ( $Q$ ). A constant bandwidth (10Hz) digital tracking filter was used with a linear sweep rate of 0.50 Hz per second in the signal processing to compute  $Q$ . The amplification factor was established at the frequency where the phase was measured to be 90 degrees.

In the beginning of the testing, it was noted that the amplification factor would change (increase) if subsequent sweeps were made for a particular normal clamping force. This initially generated concern that the rollers were moving and changing the pressure distribution within the shear interface. Specially designed alignment hardware were used to establish the position of the rollers with respect to the two halves of the test specimens and checks of the positions after a number of sweeps revealed that the rollers were not changing position. Scribe lines were made on the specimens and revealed no macro-slip between the specimens that might explain the change in the response. The most discouraging aspect of this effect was that after a higher level force test was performed, the results at a lower level could never be repeated; the  $Q$  was always higher (less damping) than for the initial sweep.

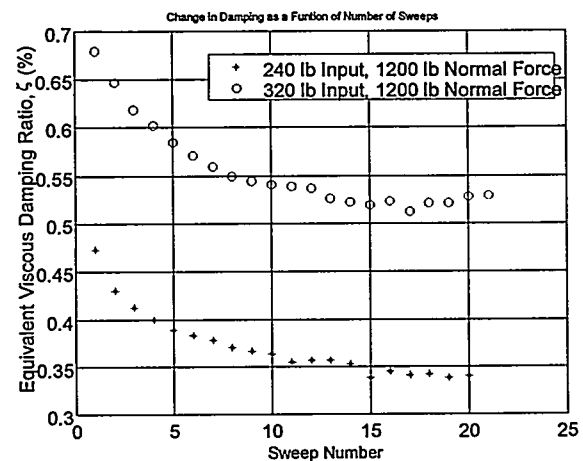
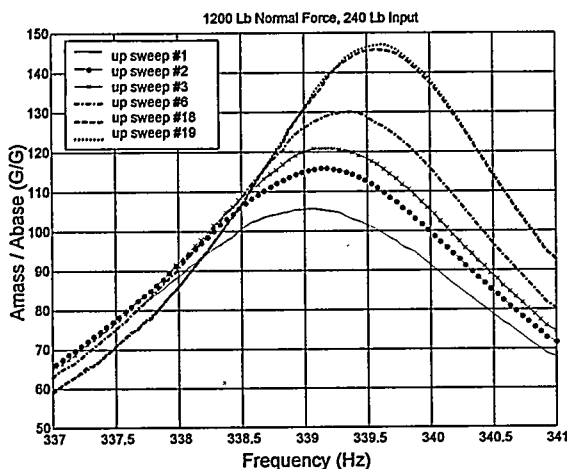


Figure 4. Change in Resonance Curves with Sweep Number

Figure 5. Change in Damping with Increasing Sweeps

This effect is shown in Figure 4 where the change in resonance curves for subsequent sweeps is illustrated. The change in the resonance curve is most pronounced for the first few sweeps and then tends to stabilize about a final



condition after many sweeps. The equivalent viscous damping ratio was also computed and plotted in Figure 5 for two load cases as a function of the sweep number, which is related to the number of cycles of vibration. The decrease in damping is also accompanied by a slight increase in the resonant frequency as if the surfaces are tending to lock up as the vibration progresses and gradually approaches a steady state. After many unsuccessful trials in search of some repeatability, it was decided to break the interface and reestablish the surface contact after each sweep. We then found that we could achieve repeatable results for a particular test configuration of a particular normal force and input force level for the initial sweep. Upon further examination of the literature, this same phenomenon was reported by other authors [9,10,15] for their experiments. The authors also noted as we did that even after many cycles of vibration the surfaces could be reestablished and similar results achieved even though there has to be some wear occurring. The evolution of the damping was fairly repeatable, similar damping was observed for the initial sweeps after reestablishing the surfaces, and the subsequent changes were also similar. This phenomenon will be further examined in future studies. The experimental results, which are presented for the remainder of the paper, were taken for the initial sweep after the surfaces were reestablished after each experiment. The surfaces were initially cleaned with a solvent and were cleaned with compressed air during each reset of the surfaces.

The amplification factors were measured for each load sequence for a selected normal force established by tensioning the cables while observing the load in each cable measured with force transducers. The amplification factors were used to compute the equivalent viscous damping ratios and the results are shown in Figure 6 as a function of the input force. The data plotted on a log-log plot approach a straight line and the slope of a straight-line fit, denoted by  $s$  on the plot legends, is computed which ranges from 0.59 to 0.83. The slope of the damping ratio for the solid bar is essentially zero which indicates a linear system response over these force ranges.

The amplification factors were then used in Equation 7 to compute the energy loss per cycle and the results are shown in Figure 7. The data show the anticipated straight line on a log-log plot indicating there exists a power law relationship between the energy loss per cycle and the input force for given normal force. The data are fit with a straight line and the slopes are shown ranging from 2.56 to 2.86. The slope of the solid bar data is almost exactly 2.0 which is what is expected for a linear system.

The data for the energy dissipation are also shown plotted on a linear plot in Figure 8 which emphasizes the relative amplitudes of the energy loss per cycle as a function of input force level. It also shows the dramatic increase in energy loss created by the presence of the friction interface when compared to the solid bar data. The data are also plotted in Figure 9 as a function of the non-dimensional force,  $F/N$ , obtained by dividing the input force by the normal force. The data lie within a band, but do not collapse to a single curve indicating that the data are not simply a function of the non-dimensional force and other parameters are required in the relationship between the input force, normal force, and energy loss per cycle. It is hoped that this relationship will be more fully understood with further study in the future.

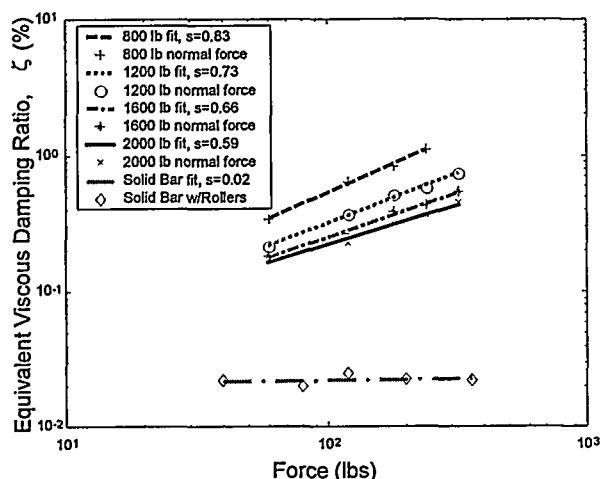


Figure 6. Equivalent Viscous Damping Ratio

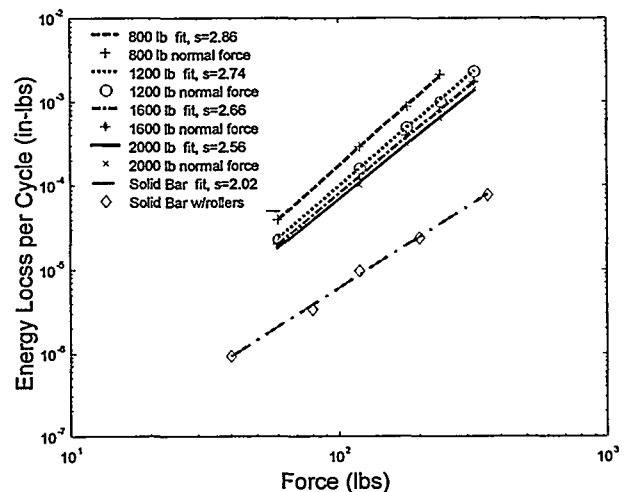


Figure 7. Energy Loss Per Cycle

Time history data was also collected for sinusoidal dwells at resonance to compute the energy loss per cycle by constructing the classical hysteresis curves. As mentioned earlier the accelerometer data was fit with the fundamental and seven harmonics and integrated to obtain the velocity and displacement. Figure 10 shows the traditional hysteresis curve of force vs. relative displacement for 1200 lb. normal force and an input force of 320 lb. The hysteresis curve shows most of the dissipation occurs near the center of the curve while the ends are very compressed indicating small dissipation in these regions. The integration of this curve yields an energy loss of almost the exact same value obtained using the amplification factor in Equation 7.

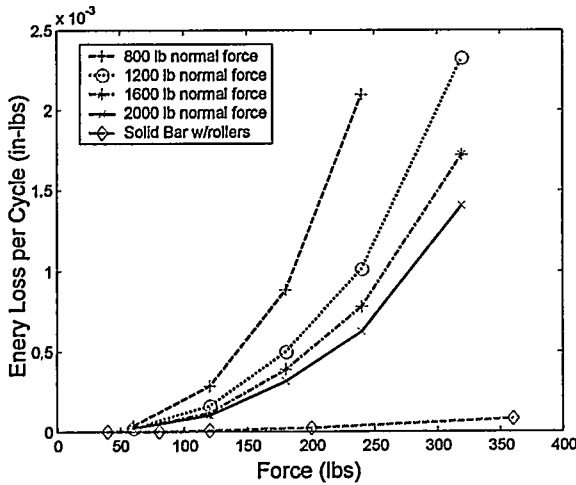


Figure 8. Linear Plot of Energy Loss Per Cycle

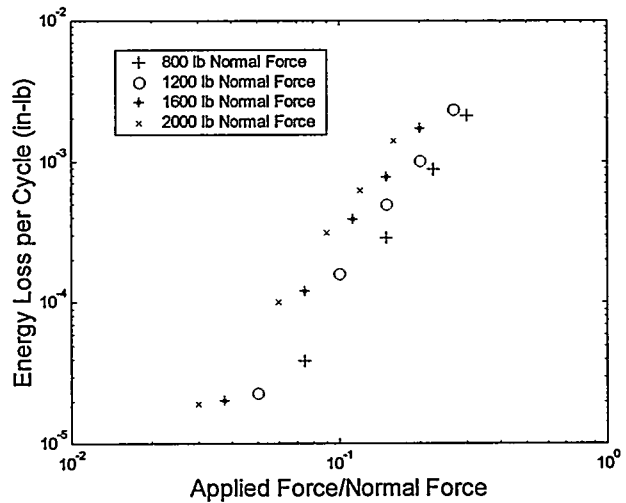


Figure 9. Energy Loss per Cycle as a Function of the Non-Dimensional Input Force

For the base excited system, another hysteresis curve can be constructed by plotting the force vs. the absolute motion of the base. As discussed earlier this hysteresis curve should yield the same energy loss per cycle as the hysteresis curve generated for the relative motion since the motion of the mass is in phase with the force and the only out of phase response is the base motion. Calculations of the energy loss per cycle by the three methods are in close agreement and are shown in Table 1. The numbers in the table are not exactly the numbers in the figures because they were taken from different data sets.

Input Force (lb.)	Q Method (in-lb.)	Relative Hysteresis (in-lb.)	Base Hysteresis (in-lb.)
120	$1.34 \times 10^{-4}$	$1.30 \times 10^{-4}$	$1.29 \times 10^{-4}$
180	$3.66 \times 10^{-4}$	$3.60 \times 10^{-4}$	$3.62 \times 10^{-4}$
240	$8.33 \times 10^{-4}$	$8.17 \times 10^{-4}$	$8.16 \times 10^{-4}$
320	$2.08 \times 10^{-3}$	$2.04 \times 10^{-3}$	$2.04 \times 10^{-3}$

Table 1. Comparison of Energy Dissipation Calculations, 1200 lb. Normal Force

At the fixed base resonance, the motion of the base to maintain a steady state response with a prescribed force is very small for a lightly damped system and without an analytical fit to the data, this hysteresis could not be constructed due to signal to noise problems. Utilizing the analytical fit, the force vs. base motion hysteresis curves shown in Figure 11 demonstrate some intriguing qualities. As discussed earlier, a linear response would exhibit an ellipse and as seen in the plot the curves deviate significantly from ellipses. The deviation from a linear response is shown in Figure 12 where the data for 1200 lb. normal force and an input force of 320 lb. is plotted with only the component at the fundamental frequency yielding an ellipse compared with the data retaining all seven harmonics in the response. The energy was computed by integrating both curves and very close agreement was achieved

indicating that almost all of the energy is dissipated at the fundamental frequency. The higher harmonics are a result of and contain information regarding the non-linear response of the system.

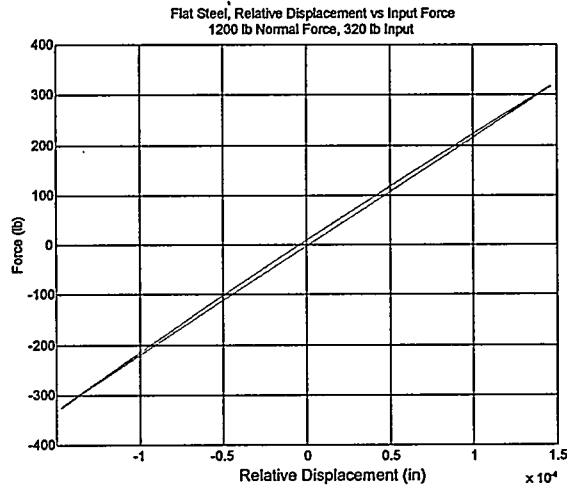


Figure 10. Relative Displacement Hysteresis Curve at Resonance

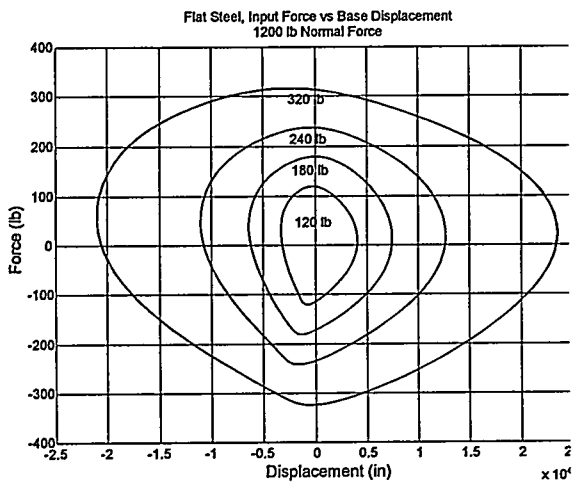


Figure 11. Base Motion Hysteresis Curves at Resonance

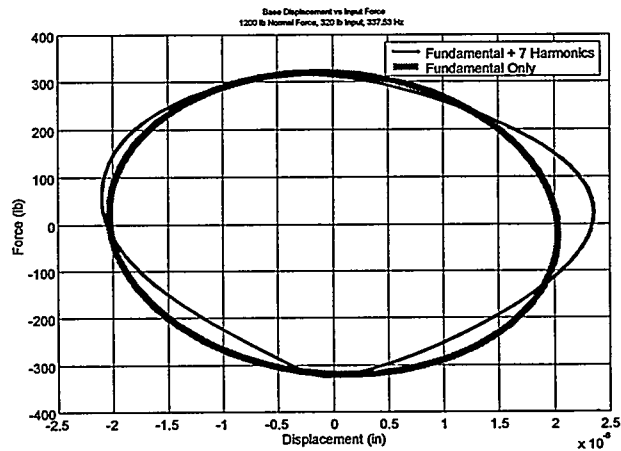


Figure 12. Comparison of Hysteresis with only Fundamental Frequency Component with Hysteresis Computed Retaining Seven Harmonics

### SUMMARY AND CONCLUSIONS

An experiment has been described for determining the energy loss mechanism in a frictional joint in shear. The experiments are yielding insights into the physics of the microslip phenomenon and the associated damping mechanism. Several pitfalls in making these measurements were described. It was shown that several different methods for measuring the energy loss in the joint yield essentially the same result. It was shown that an equivalent viscous damping coefficient could be measured that describes the energy loss in the joint. An efficient way to measure the energy loss was developed which uses the transmissibility curve near the fixed base resonant frequency of a single-degree-of-freedom system. Performing the experiments at resonance offers several advantages. First the phase difference between the force and motion becomes much more measurable since it approaches 90 degrees at resonance. At resonance, the mass and inertia forces balance and the damping force (albeit it very small) is isolated and can be directly observed. The measurement of the amplification factor,  $Q$ , at resonance allows the energy loss per cycle to be calculated without the need to difference accelerometers. At the fixed base resonance, the energy

supplied to the system is equal to the energy dissipated in the system to sustain steady state response. The harmonics of the response contain the non-linear portion of the response and contain information regarding the physics of the microslip phenomenon. This information should prove valuable to researchers attempting to build physics based models of a joint.

The data indicate a power law relationship typically applies to the energy losses in the joint. For the material and loading conditions we measured, slopes on a log-log plot of energy loss/cycle vs. force were from about 2.5 to 2.9. The data show that the slope increases slightly as the normal force is relaxed. It also was shown that this measurement gave essentially equivalent results as integrating both the relative displacement and base displacement hysteresis curves. Using  $Q$ , the equivalent viscous damping ratio can also be computed and plotted as a function of the input force. It was shown that this data also falls on a straight line on a log-log plot and the slope of this plot is directly related to the slope of the energy dissipation curve.

Much work needs to be done. We need to investigate the functional form of the observed nonlinearities. We still need to investigate the influence of several parameters including-- materials, surface finish, frequency, a larger range of force levels, different interface pressure distributions, and non-periodic excitation. The change in the damping as a function of the number of vibration cycles also needs to be investigated further. In future experiments, we intend to include a bolt to see if the information gathered for the simple shear interface can be extended to the more complicated case of a bolted joint. The removal of the linear part of the response to isolate the nonlinear portion will be further investigated to help develop models to capture the nonlinear system response.

#### REFERENCES

1. Goodman, L.E. "A review of progress in analysis of interfacial slip damping", *Structural Damping*, papers presented at a colloquium on structural damping held at the ASME annual meeting in Atlantic City, NJ, December, 1959, edited by Jerome E Ruzincka, pp 35-48.
2. Goodman, L. E. and Brown, C. B., "Energy Dissipation in Contact Friction: Constant Normal and Cyclic Tangential Loading", *Journal of Applied Mechanics*, pp. 17-22, 1962.
3. Ungar, E. E., "The Status of Engineering Knowledge Concerning the Damping of Built-Up Structures", *Journal of Sound and Vibration*, 26, August, 1977, pp. 141-154.
4. Methereil, A. F. and Diller, S. V., "Instantaneous Energy Dissipation Rate in a Lap Joint – Uniform Clamping Pressure", *Journal of Applied Mechanics*, 35, March 1968, pp. 333-340.
5. Groper, M., "Microslip and Macroslip in Bolted Joints", *Experimental Mechanics*, June, 1985, pp. 171-174.
6. Menq, C.H., Bielak, J., and Griffin, J. H., "The Influence of Microslip on Vibratory Response, Part 1, A New Microslip Model", *Journal of Sound and Vibration*, 107, 1986, pp 279-293.
7. Gaul, L. and Lenz, J., "Nonlinear Dynamics of Structures Assembled by Bolted Joints" *ACTA Mechanica*, 125, April, 1997, pp. 169-181.
8. Sanliturk, K. Y., Stanbridge, A. B., and Ewins, D. J., "Friction Dampers: Measurement, Modelling and Application to Blade Vibration Control", ASME Design Engineering Technical Conferences, Volume 3, Part B, 1995.
9. Rogers, P. F. and Boothroyd, G. "Damping at Metallic Interfaces Subjected to Oscillating Tangential Loads", *Transactions of the ASME, Journal of Engineering for Industry*, August, 1975, pp. 1087-1093.
10. Padmanabhan, K. K. and Murty A. S. R., "Damping in Structural Joints Subjected to Tangential Loads", *Proceedings of Institution of Mechanical Engineers*, Vol. 205, pp. 121-129, 1991.
11. Harris, C. M. *Shock and Vibration Handbook*, 4<sup>th</sup> edition, Eq. 2.41, McGraw-Hill, New York, NY, 1996.
12. Thomson, W. T., *Vibration Theory and Applications*, Prentice-Hall, Englewood Cliffs, NJ, 1965.
13. D. L. Gregory, D. O. Smallwood, R. G. Coleman, M. A. Nusser, " Experimental Studies to Investigate Damping In Frictional Shear Joints," *Proceedings of the 70<sup>th</sup> Shock and Vibration Symposium* (1999).
14. D. L. Lobitz, D. L. Gregory, and D. O. Smallwood, "Comparison of Finite Element Predictions to Measurements from the Sandia Microslip Experiment," Accepted for presentation at IMAC, 2001.
15. Vitelleschi, S. and Schmidt, L. C., "Damping in Friction-Grip Bolted Joints", *Journal of the Structural Division, Proceedings of ASCE*, Vol. 103, No. ST7, J